Int. j. adv. multidisc. res. stud. 2024; 4(2):717-723

Received: 07-02-2024
Accepted: 17-03-2024

International Journal of Advanced Multidisciplinary Research and Studies

ISSN: 2583-049X

Microstructure and Mechanical Properties of Electric arc welded Low-alloy Steel at Varied Welding Heat Input

[1] Kutelu BJ, [2] Ogundeji FO, [3] Aluko AO

[1, 2, 3] Department of Mineral and Petroleum Engineering Technology, The Federal Polytechnic, Ado-Ekiti, Ekiti, State, Nigeria

Corresponding Author: **Ogundeji FO**

Abstract

In fusion welding technique, heat input has a significant effect on the microstructure and mechanical properties of the welded joint. In this study, effects of varied welding heats on the microstructure and mechanical properties of low-alloy steel were investigated using electric arc welding technique. Optical emission spectrometry (AR 4 30 metal analyzer) was used to determine the chemical composition of the as-received low alloy steel sample. Based on ASTM A778/778M, five butt-joint samples were produced at different voltages, and constant speed and current. A portion of the welded sample was prepared by conventional metallographic grinding and polishing techniques for metallurgical examination using Philips SEM (XL30 TMP). The remaining portions were machined to standard tensile and hardness and impact specimens, using lathe machine. The tensile and hardness specimens were prepared in accordance with ASTM E 8-04 standard and the impact specimen based on ASTM A370 standard. The test specimens were subjected to mechanical testing using INSTRON tensile testing machine, digital Rockwell hardness scale B (HRB) and Charpy impact tester respectively. Results obtained revealed microstructures with varied volume fraction of ferrite, interspersing the austenite matrix. Pearlite and martensite phases were also sparsely dispersed within the austenite matrix. In addition, microstructures of the weldments were characteristically inhomogeneous, and at high heat inputs, increased presence of precipitates were seen within the microstructures. Maximum tensile properties (UTS, 498MPa, YS, 329 MPa) were obtained at heat input of 17.43 J/mm and least tensile properties (UTS, 469MPa, YS, 312 MPa) were obtained at 857.14 J/mm; maximum hardness property (484HRB) and least hardness property (394HRB) were obtained at 171.43 J/mm and 857.14 J/mm respectively; maximum impact energy (112.02 J) and least impact energy (88.79 J) were obtained at 514.29 J/mm and 857.14 J/mm respectively.

Keywords: Fusion Welding, Butt-joint, Weldment, Microstructures, Heat Inputs, Volume Fraction, Low Alloy Steel

1. Introduction

Low-alloy steels are a category of ferrous materials with mechanical properties superior to plain carbon steels, because of additions of alloying elements such as nickel, chromium and molybdenum. The total alloy content of low alloy steels can range from 2.07% up to levels just below that of stainless steels, containing a minimum of 10% Cr (Gharishahiyan *et al.*, 2011 [14]; Lancaster, 2003; Agarwal, 1992 [3]). Low alloy steels are used for a wide range of applications, including offshore and onshore structural engineering plates, pipes, automotive and aerospace bodies and railway lines (Agarwal, 1992) [3].

Welding is a traditional method of joining steel materials. During welding, the base metal experiences a range of temperature invariably from fusion to melting, depending on the cooling rate and steel composition, base metal close to the fusion area is transformed to austenite, martensite, ferrite and bainite. These different phase microstructures correspond to different mechanical properties (Chellappan *et al.*, 2016; Bourmerzoung *et al.*, 2010; Kožuh *et al.*, 2009; Afolabi, 2008) [10, 8, 17, 2]. Generally, a weld exhibits coarse crystal structure relative to the parent metal, which is in the wrought condition, the presence of some elements in steel such as chromium accelerate grain growth. As a result, large grain is produced in the metal near to the weld (Apurv *et al.*, 2014; Kožuh *et al.*, 2009; Ghosh *et al.*, 2006) [4, 17, 15]. Welding voltage, current, stick out, wire feed rate and welding speed are some of the independent controllable process parameters, affecting mechanical properties (Abioye, 2017; Oyetunji *et al.*, 2013; Bourmerzoung *et al.*, 2010) [1, 20, 8].

Past research findings have shown that the dimension of the heat affected zone (HAZ) layers of a submerged arc welded (SAW) low- alloy steel was increased with increase in welding voltage and decreased with increase in welding speed. Also, the dimension was increase with increasing in wire feed rate and heat input (Dibit *et al.*, 2019) [12]. And according to Sindo, (2003) [24] arc length is primarily controlled by welding voltage, with increase in welding voltage, bead flattened out more and width-to-depth ratio is increased. In fusion welding, both mechanical and metallurgical properties of the weld joint are significantly influenced by welding heat input, and if, welding heat input is not controlled, it could lead to undesirable microstructures, and hence, mechanical properties.

Therefore, efforts were made in this work to assess the performance of electric arc welded low alloy steel produced at varied heat inputs, this is with the aim of obtaining optimum welding heat input for the joint production under different loading conditions.

2. Materials and Method

2.1 Materials

The low alloy steel used for the study and electrode were obtained from Universal Steel Ltd. Ogba, Lagos, Lagos and relevant vendor respectively. The Chemical composition of the experimental low alloy steel was determined using optical emission spectrometry (AR 4 30 metal analyzer). The sample was ground, mounted on the sparkling point of the spectrometer and sparked three (3) times. Mean value of the detected elements was recorded and reported in Table 1.

Table 1: Chemical Composition of the low alloy steel (wt. %)

Element	C	Si	Mn	S	P	Cr	Ni	Cu	Al	Mo	V	Fe
Wt. % Comp	0.18	0.51	0.54	0.01	0.03	5.12	0.24	0.14	0.02	0.55	0.08	

2.2 Method

2.2.1 Welding

The weld samples, comprising of butt joint and single V configuration were prepared, and the weld joints were produced at varied range of electric arc welding voltage in accordance with ASTM A778/778M (2016) standard. Tables 2 depicts procedure for the weldments production, and Eqn. 3.1 was used to calculate the welding heat inputs.

Table 2: Weldment production procedure

S. No	Voltage (V)	Current (A)	Speed (mm/s)
1	5	120	3.5
2	10	120	3.5
3	15	120	3.5
4	20	120	3.5
5	25	120	3.5

$$Q = \frac{VI}{S} \quad (1)$$

Where,

Q is heat input (J/mm);
Vis the voltage (V);
I is the current (A); and
S is the speed (mm/s)

2.3 Scanning electron microscopy (SEM)

SEM samples were prepared by the conventional metallographic grinding and polishing techniques. This was followed by colloidal silica polishing. Philips SEM (XL30 TMP) was used to further characterize the samples.

2.4 Mechanical Testing

2.4.1 Tensile test

Specimens used for the tensile test were prepared in accordance with ASTM E 8-04. The specimens were machined to 3.5 mm diameter (⌀) and 32 mm gauge length (L), and placed in the proper grippers of INSTRON tensile testing machine- model 3369 load was applied at the rate of 0.5mm/min.

2.4.2 Hardness

Samples of dimension 15 mm length, 10 mm breadth, and 8 mm thickness was used for the hardness test. Surfaces of specimens were properly ground to make them flat and stable, using hand grinder. The specimens were prepared in accordance with ASTM E 8-04 standard. Hardness measurement was made using Digital Rockwell hardness scale B (HRB). And in order to obtain zero position, a minor load, weighing 10Kgf was applied to the surface of the specimens with a dwell time of 10 seconds.

And upon establishing the zero position, a heavier major load, weighing 60 Kgf was then applied to the specimens, leading to indentation. The minor load was maintained all throughout the test. Due to some variations of the test, the major load was allowed to remain on the specimens until the indent it has made is deep enough. Thereafter, the major load was removed, and the depth of the penetration, starting from the zero position was measured. For each of the specimen, indentation were made in three different locations, using diamond pyramid and the average values were recorded, and depicted in Table 1 is the result.

2.5 Impact energy

Specimens used for the Charpy impact test were prepared based on ASTM A370 standard. The specimens were machined to 55 mm length, 10 mm breadth and 10 mm thickness with a V-shape notch of depth 4.5 mm across the larger (55 mm length) dimension. One end of the specimens was fixed in a cantilever position by means of a vice. Weighed pendulum with hammer was dropped from a fixed height to make contact with the specimens. The hammer strike opposite the notch, and the energy absorbed by the specimens was determined by measuring the decrease in motion of the pendulum.

3. Results and Discussion

3.1 Analysis of chemical composition of the low-alloy steel sample

The as-received experimental low alloy steel is comprised of 5.12 % Cr, 0.55% Mo, 0.54% Mn, 0.24% Ni and 0.18% C (Table 1), indicating that it is of BS1503 standard and grade 625.

3.2 Scanning Electron Microscopy (SEM)

From SEM micrograph of the as-received low alloy steel sample (Plate 1), the microstructure is characterized by varied volume fraction of austenite phase (dark portion) and ferrite phase (light portion), which are the major phases, which was attributed to thermal history of the sample. In addition, presence of pearlite and cementite phases of varying grain sizes are palpable (Oyetunji *et al.*, 2013; Lichan *et al.*, 2013; Kožuh *et al.*, 2009) [20, 19, 17].

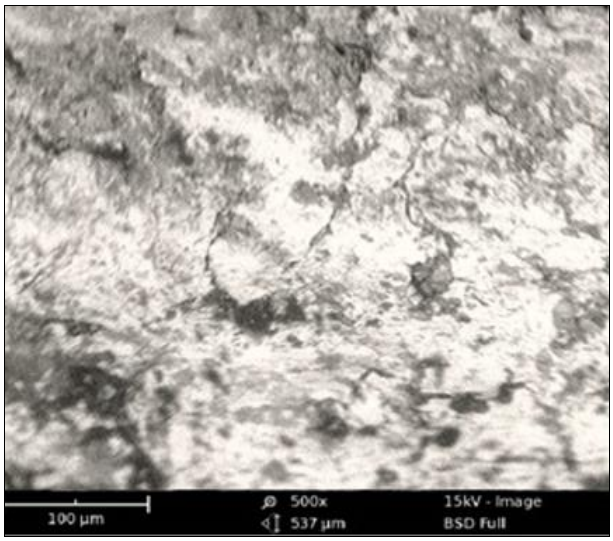

Plate 1: SEM micrograph of the as-received low alloy steel sample

Plates 2, 3, 4, 5 and 6 are SEM micrographs of the welded low alloy steel at the varied heat inputs of 171.43 J/mm, 342.86 J/mm, 514.29 J/mm, 685. 71 J/mm and 857.14J/mm respectively. The microstructures are heterogeneous, which may have resulted from the temperature gradient that resulted during the weldments production (Oyetunji *et al.*, 2013; Subodh and Shahi, 2011; Kozuh *et al.*, 2009) [20, 25, 17]. And they are comprised of austenite and ferrite as the major phases. In comparison, grain sizes of the austenite and ferrite phases are coarse relative to those of the as-received low alloy sample. At the varied heat inputs, average grain sizes of FZ microstructures are finer as compared to the corresponding HAZ microstructures. And at increased heat inputs, grain coarsening resulted, because cooling rate was slow, allowing sufficient time for grain growth, and at low heat input, cooling rate was fast, grain growth suppression as a result of insufficient time that was provided for grain growth (Pauli *et al.*, 2016; Tabish *et al.*, 2014 [26]; Calik, 2009 [9]). Also, observed within the microstructure were pearlite and cementite phases, which were sparsely dispersed in varied volume fraction within the austenite matrix (Gharishahiyan *et al.*, 2011) [14].

In addition, dark spots that are apparent within the microstructures at the varied heat inputs are inclusions that resulted from chemical reactions that resulted between alloying elements and non-metallic elements such S and C (Coata, 2018) [11]. And the tiny particles that were seen within the microstructures were due to alloying elements, including Mn, Si, Al, Mo and Ti that reacted with oxygen in the weld pool at high the temperature of the electric arc welding process, during which, a single-phase oxide (MnO - SiO_2 - Al_2O_3) may have been formed (Bhatti *et al.*, 1984) [6].

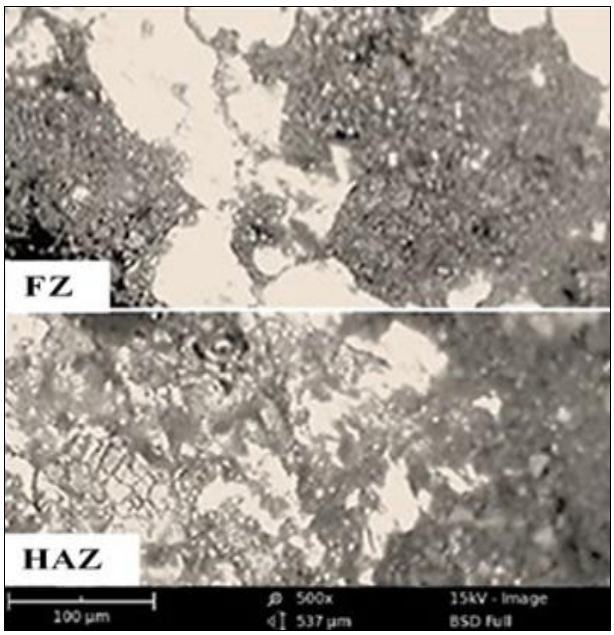

Plate 2: SEM micrograph of the low alloy steel weldment at 685.71J/mm heat input

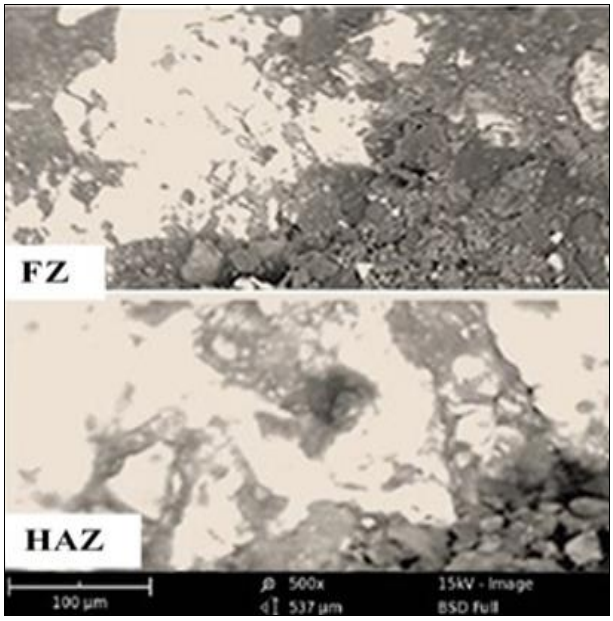

Plate 3: SEM micrograph of the low alloy steel weldment at 342.86 J/mm heat input

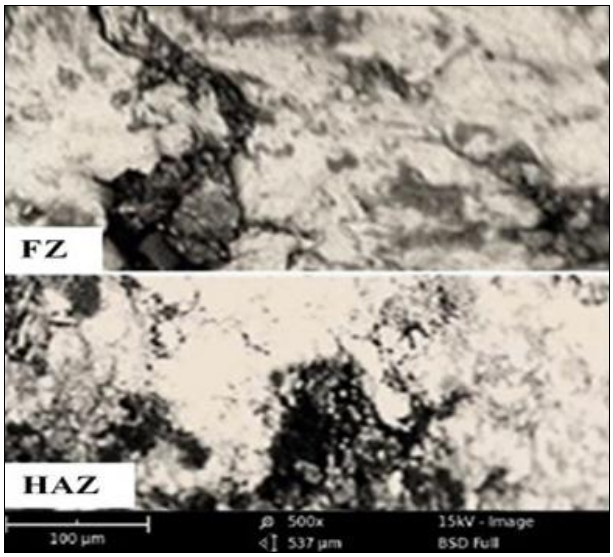

Plate 4: SEM micrograph of the low alloy steel weldment at 514.29 J/mm heat input

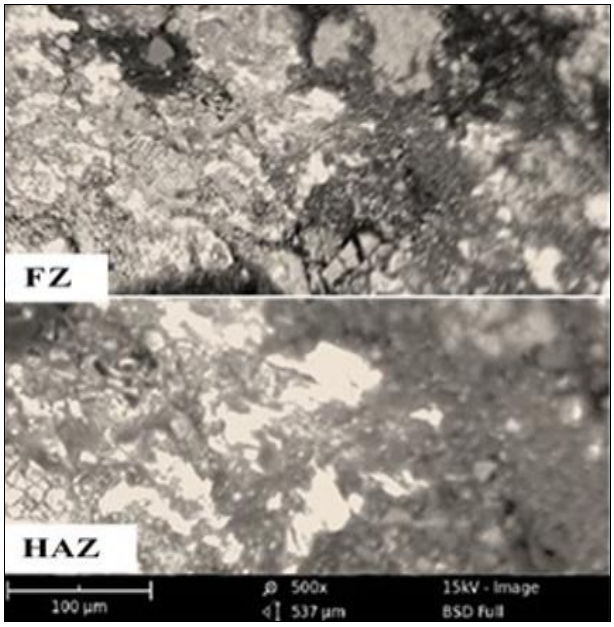

Plate 5: SEM micrograph of the low alloy steel weldment at 171.43 J/mm heat input

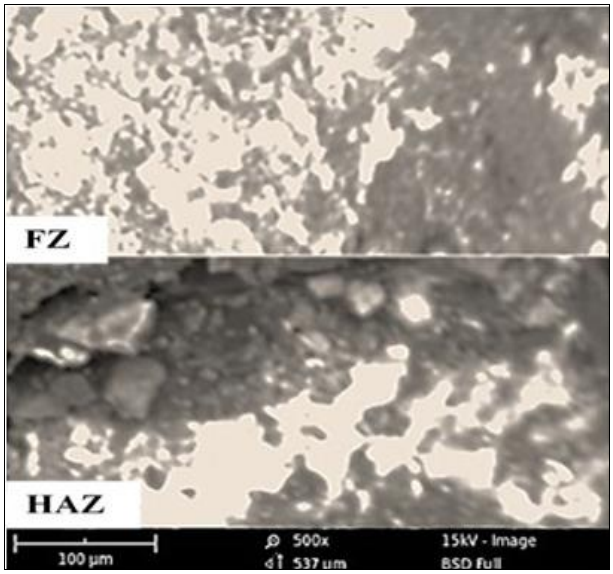

Plate 6: SEM micrograph of the low alloy steel weldment at 857.14 J/mm heat input

3.3 Mechanical Testing

Tensile properties

Figs. 1, 2 and 3 are the UTS, YS and %E of the sample at the varied heat inputs of 0.0 J/mm, 171.43 J/mm, 342.86 J/mm, 514. 29 J/mm, 685. 71 J/mm and 856.14 J/mm. The superior tensile properties (YS and UTS) at heat inputs range of 171.43-514.29 J/mm as compared to 685. 71-857.14 J/mm was partly as a result fast cooling conditions that accompanied the electric arc process. Consequently, smaller grains were produced, leading greater ratio of grain boundary to dislocation with concomitant increased hindrance of dislocation motion. On the other hand, inferior tensile properties (YS and UTS) at heat inputs range of 685. 71- 857.14 J/mm can be attributed to coarser grains that resulted from slow cooling conditions, leading to less grain boundaries and hindrance to dislocation motion (Pauli *et al.*, 2016; Kondapalli *et al.*, 2011; Ghosh *et al.*, 2006 [15]).

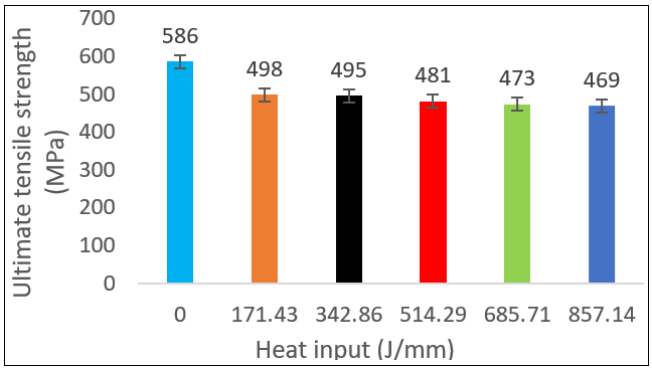

Fig 1: Tensile characteristic (UTS) of the as-received and welded low- alloy steel samples at varied heat input

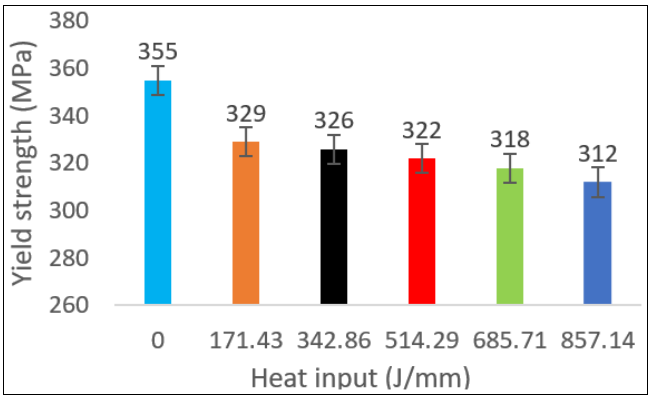

Fig 2: Tensile characteristic (YS) of the as-received and welded low- alloy steel samples at varied heat input

Hardness property

Fig 3 depicts hardness properties at the varied heat input range. It is obvious from the result, that hardness property was decreased with increasing heat input. The superior hardness of the weldment at heat input range of 171.43-514.29 J/mm relative to 685. 71 - 857.14J/mm is attributable to grain size differential (Xio - Long *et al.*, 2018; Hassen, 2004) [28, 16]. At the later range of heat input, grain growth was suppression of grain growth was accentuated by the fast-cooling conditions of the electric arc welding process. While at the later range of heat input, grain growth was enhanced by the slow cooling conditions. Past researchers have attributed superior and inferior hardness property to fine and coarse grains respectively (Behnam *et al.* [7], 2019; Pauli *et al.*, 2016; Hassen, 2004) [16].

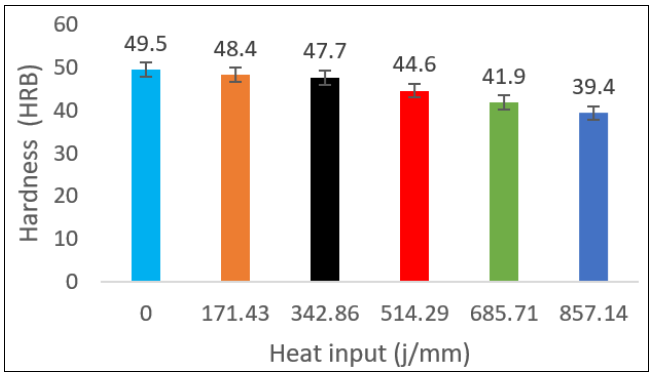

Fig 3: Hardness characteristics of the as -received and welded low-alloy steel samples at varied heat input

Impact energy

Fig 4 depicts impact energy behaviour of the low alloy steel at the varied heat inputs. In general, increase in grain size raises impact failure transition temperature by brittle fracture (Yonghe *et al.*, 2015) [31]. Therefore, the observed variations in impact energy of the weldments at the varied range of heat inputs were partly due to grain size effect. In addition, differences in phase distribution, inclusions and tiny particles within the microstructures may be contributory (Apurv, and Vijaykumar, 2014; Bourmerzoung *et al.*, 2010) [4, 8]. And due to coarse grains at heat input range of 685. 71-857.14 J/mm, there is the possibility of increased presence of voids and micro cracks, which may have partly resulted in the poor impact performance of the weldment (Zakaria *et al.*, 2010) [32]. Also, the presence impurities, segregating at the grain boundaries could be more at this range, which may be a factor as well (Fowless and Blake, 2008) [13].

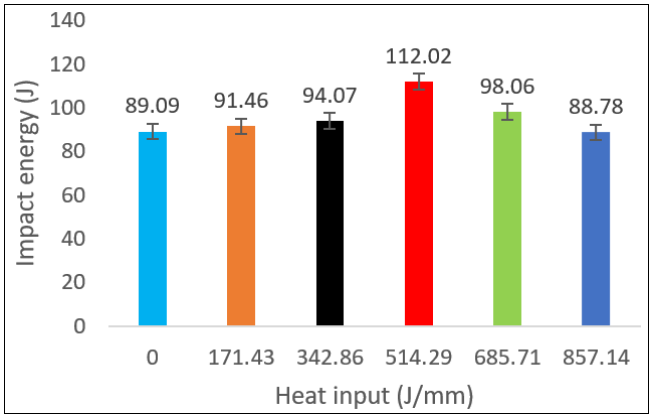

Fig 4: Impact characteristics of the as-received and welded low-alloy steel samples at varied heat input

4. Conclusions

Based on the results of the work, the following conclusions were drawn:

1. Microstructure of as-received low alloy sample is comprised predominantly of austenite and ferrite. Other phases are pearlite and martensite.
2. Microstructures of the welded samples are heterogeneous, comprising of varied volume fraction of ferrite, interspersing austenite matrix. And increased presence of precipitates were revealed by microstructures of the welded samples that were produced at the ranges welding voltage that favour high heat inputs
3. UTS, YS and %E properties of the as-received low-alloy steel sample with values of 586 MPa, 355 YS and 52% respectively were superior relative to UTS, YS and %E properties of the welded low alloy steel sample.
4. Optimum UTS and YS properties of the welded low-alloy sample of 498 MPa and 329MPa respectively were obtained at 171.43J/mm heat input, while the corresponding least UTS and YS of the welded low alloy sample of 469 MPa and 312 MPa respectively were obtained at 857.14 J/mm heat input.
5. Optimum hardness property of 48.4 HRB and least hardness property of 39.8HRB were revealed by the welded sample. However, the hardness property of 49.5 HRB shown by the as-received sample was high relative to the optimum hardness property of the welded sample.
6. Impact energy property of the welded sample was superior to impact energy property of the as-received sample at the range (171.43 – 685.71 J/mm heat input) and superior to impact energy property of the as-received sample at 857.14 J/mm heat input.

5. References

1. Abioye TE. Effect of heat input on the mechanical and corrosion properties of AISI 304 electric arc weldments. British Journal of Applied Science and Technology. 2017; 20.
2. Afolabi AS. Effect of electric arc welding parameters on corrosion behaviour of austenitic stainless steel in chloride medium. AU Journal of Technology. 2008; 11(3):171-180.
3. Agarwal RL. Welding engineering- A textbook for engineering students, Khanaa Publ., Sarai, Delhi, India, 1992, 56-62.
4. Apurv C, Vijaykumar SJ. Influence of heat input on mechanical properties and microstructure of austenitic 202 grade stainless steel weldments. WSEAS Transactions on Applied and Theoretical Mechanics. 2014; 9:222-228.
5. Armentani E, Esposito R, Sepe R. The effect of thermal properties and weld efficiency on residual stresses in welding. Journal of Achievements in Materials and Manufacturing Engineering. 2007; 20(1-2):319-322.
6. Bhatti AR, Saggese ME, Hawkins DN, Whiteman JA, Golding MS. Analysis of inclusions in submerged arc welds in micro alloyed steels. Welding Journal. 1984; 63(7):224-230.
7. Behnam S, Hassan S, Mahdi R, Ahmad Reza A, Ehsan S. Microstructural, mechanical and corrosion properties of dissimilar joint between AISI a321 stainless steel and ASTM A537CL1 structural steel produced by GTAW process. Metall. Res. Technol. 2019; 116(4):145-157.
8. Bourmerzoung Z, Derfouf G, Baudin T. Effect of welding on microstructure and mechanical properties of an industrial low carbon steel. Engineering. 2010; (7):502-506.
9. Çalik A. Effect of cooling rate on hardness and microstructure of AISI 1020, AISI 1040 and AISI 1060 steels. Int. J. of Phys. Sci. 2009; 4(9):514-518.
10. Chellappan M, Ligadurai KSP, Devakumaran K, Raja K. Effect of heat input on mechanical and metallurgical properties of gas tungsten arc welded lean super martensitic stainless steel. Material Research. 2016; 19(3):572-579.
11. Costa S. Non-metallic inclusions in steels - origin and

control (Review). J. Mater Res Technol, 2018, 283-299.
12. Dibit Sumardiganto, Sri Endah Susilowati. Effect of welding parameters on mechanical properties of low carbon steel API 5L shielded metal arc welds. American Journal of Materials Science. 2019; 9(1):15-21.
13. Fowless RJ, Blake SE. Influence of heat input on austenitic stainless steel. Weld Properties African Fusion. 2008; 1(2):17-24.
14. Gharishahiyan E, Raouf AH, Parvin N, Rahimian M. The effect of microstructure on hardness and toughness of low carbon welded steel using inert gas welding. Materials and Design. 2011; 32(4):2042-2048.
15. Ghosh A, Das Su, Chatterjee S, Ramchandra Rao P. Effect of cooling rate on structure and properties of an ultra-low carbon HSLA-100 grade steel. Mater Charact. 2006; 56:56-65.
16. Hansen N. Hall–Petch relation and boundary strengthening. Scr Mater. 2004; 51:801-806.
17. Kožuh S, Goji´c M, Kosec L. Mechanical properties and microstructure of austenitic stainless steel after welding and post-weld heat treatment. Kovove Mater. 2009; 47:253-262.
18. Lee JI, Um KW. A prediction of welding process parameters by prediction of back-bead geometry. Journal of Materials Processing Technology. 2000; 108(1):106-113.
19. Lichan Li, Menngyu Chai, Yongquann li, Wenjie Bai, Quan Duan. Effect of heat input on grain size and microstructure of 316L stainless steel welded joint. Applied Mechanical and Material. 2013; 331:578-582.
20. Oyetunji O, Kutelu BJ, Akinola AS. Effects of welding speeds and power inputs on the hardness property of Type 304 Laustenitic stainless steel heat-affected zone (HAZ). Journal of Metallurgical Engineering (ME). 2013; 2 I:124-129.
21. Patil SC, Waghmare C. Optimization of MIG welding parameters for improving strength of welded joints. International Journal of Advanced Engineering Research and Studies. 2013; 2:14-16.
22. Romans P, Simons EM. Welding processes and technology. Pitman Pub. New York. 2002; 34.
23. Sadat AR. Effect of heat input on the microstructure and mechanical properties of a weld joint- A review. Journal of Applied Engineering and Research. 2018; 13(6):184-188.
24. Sindo K. Welding Metallurgy, Second Edition, John Wiley and Sons, Inc., Hoboken, Canada, 2003.
25. Subodh Kumar AS, Shahi. Effect of heat on the microstructure and mechanical properties of gas tungsten arc welded AIAI 304 stainless joints. Materials and Design. 2011; 32:3617-3623.
26. Tabish TA, Abbas T, Farhan M, Atiq S, Butt TZ. Effect of Heat Input on Microstructure and Mechanical Properties of the TIG Welded Joints of AISI 304 Stainless Steel. International Journal of Scientific and Engineering Research. 2014; 5:1524-1532.
27. Weihua Sun, Guodong Wang, Jiming Zhang, Dianxiu Xia, Hao Sun. Microstructural characteristization of high heat input welding joint of HSLA steel plate for oil storage construction. J Mater Sci Technol. 2009; 25(6):857-860.
28. Xio - Long Gao, Jing Lin, Lin - Zhang. Effect of heat input on the microstructure and mechanical properties of pulsed laser welded joints in Ti6Al4V/N dissimilar alloy. International Journal of Advanced Manufacturing Technology. 2018; 94:3937-3947.
29. Yayla P, Kalae E, Ural K. Effect of welding processes on the mechanical properties of HY 80 steel weldments. Mater Des. 2007; 1898-1906.
30. Ying-qio Zhang, Han-qian zhang, Jin fud Li, Wei-ming Liu. Effect of heat input on microstructure and toughness of coarse grain heat-affected zone Nb microalloyed HSLA steel. J. Iron and Steel Research Inter. 2009; 16(5):73-80.
31. Yonghe Y, Lei S, Zhen X, Hongsheng L, Xu C, Xin W. Fracture toughness of the materials in welded joint of x80 pipeline steel. Engineering Fracture Mechanics. 2015; 148:337-349.
32. Zakaria B, Chemseddine D, Thierry B. Effect of welding on microstructure and mechanical properties of an industrial low carbon steel. Scientific Research Engineering. 2010; 2:502-506. Doi: 10.4236/eng.2010.27066 Published Online (http://www.SciRP.org/journal/eng)